J|A|C|S ARTICLES

Published on Web 11/13/2009

New Synthetic Procedures to *Catena*-Phosphorus Cations: Preparation and Dissociation of the First *cyclo*-Phosphino-halophosphonium Salts

Jan J. Weigand,*,† Neil Burford,*,‡ Reagan J. Davidson,†,‡ T. Stanley Cameron,‡ and Patrick Seelheim†

Department of Inorganic and Analytical Chemistry, Westfälische Wilhelms-University Münster, Corrensstrasse 30, 48149 Münster, Germany, and Department of Chemistry, Dalhousie University, Halifax, Nova Scotia B3H 4J3, Canada

Received September 10, 2009; E-mail: jweigand@uni-muenster.de; Neil.Burford@dal.ca

Abstract: Chlorination of 1,2,3,4-tetracyclohexyl-*cyclo*-tetraphosphine (**2**) by $PhICl_2$ or PCl_5 in the presence of Me_3SiOTf or $GaCl_3$ provides a stepwise approach to salts of the first *cyclo*-phosphino-chlorophosphonium cations $[Cy_4P_4Cl]^+$ ([**19**]$^+$) and $[Cy_4P_4Cl_2]^{2+}$ ([**20**]$^{2+}$). The analogous iodo derivative $[Cy_4P_4I]^+$ ([**17**]$^+$) is obtained as the tetraiodogallate salt from reaction of **2** with I_2 in the presence of GaI_3. Reactions of the dication [**20**]$^{2+}$ with PMe_3 or dmpe effect a dissociation of the cyclic framework resulting in the formation of salts containing $[Me_3PPCyPCyPMe_3]^{2+}$ ([**27**]$^{2+}$), $[dmpeCyP]^{2+}$ ([**29**]$^{2+}$), and $[dmpeCyPCyP]^{2+}$ ([**30**]$^{2+}$), respectively. The new cations represent phosphine complexes of the $[PCy]^{2+}$ and $[P_2Cy_2]^{2+}$ cationic fragments from [**20**]$^{2+}$, demonstrating the coordinate nature of the phosphinophosphonium bonds in *cyclo*-phosphino-halophosphonium cations. The compounds have been characterized by NMR spectroscopy, single crystal X-ray crystallography, and Raman spectroscopy.

Introduction

Catena-phosphinophosphonium cations represent a potentially diverse new class of compounds that represent analogues of the homoatomic frameworks of carbon.[1] The presence of a molecular cationic charge enhances the P−P bond energy and provides for high yield preparative reactions. A variety of synthetic approaches have been described. Most obvious are the single or double alkylation of a polyphosphine.[2−6] For example, diphosphines **1** are precursors to phosphinophosphonium cations **3**[3] and diphosphonium cations **5**,[2] and *cyclo*-tetraphosphines **2** are precursors to *cyclo*-triphosphino-2-phosphonium cations **4**[4,5] and cyclo-1,3-diphosphino-2,4-diphosphonium dications **6**[6] (Scheme 1).

Halogenation reactions of polyphosphines offer a potentially versatile alternative approach to cationic electrophile addition recognizing that a phosphine **7** reacts with a dihalogen, X_2, to give a P−X−X linear adduct **8**[7,8] or a halophosphonium salt **9**[9,10] (Scheme 2), depending on the basicity of the phosphine,[7,8] the basicity of the anion X^-,[11,12] and the solvent.[13] As shown in Scheme 3, halogenation of diphosphines (**1**) gives halophosphines (**10**) via adduct **11** and ion pair [**12**][X], as the presence of the halide anion X^- anion leads to the cleavage of P−P bonds by an S_N2 reaction.[14] Correspondingly, halogenation of *cyclic*-phosphines **14** by reaction with dihalogens also results in P−P bond cleavage to give dihalophosphines **16** (Scheme 4), and

Scheme 1. Sequential Alkylation of Diphosphines and Cyclophosphines

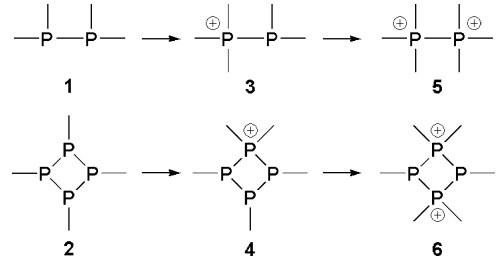

Scheme 2. Halogenation of Tertiary Phosphines

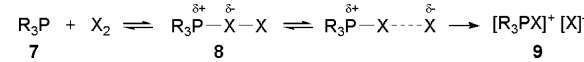

† Westfälische Wilhelms-University Münster.
‡ Dalhousie University.

(1) Dyker, C. A.; Burford, N. *Chem. Asian J.* **2008**, *3*, 28–36.
(2) Weigand, J. J.; Riegel, S. D.; Burford, N.; Decken, A. *J. Am. Chem. Soc.* **2007**, *129*, 7965–7976.
(3) Burford, N.; Dyker, C. A.; Decken, A. *Angew. Chem., Int. Ed.* **2005**, *44*, 2364–2367.
(4) Burford, N.; Dyker, C. A.; Lumsden, M. D.; Decken, A. *Angew. Chem., Int. Ed.* **2005**, *44*, 6196–6199.
(5) Dyker, C. A.; Riegel, S. D.; Burford, N.; Lumsden, M. D.; Decken, A. *J. Am. Chem. Soc.* **2007**, *129*, 7464–7474.
(6) Riegel, S. D.; Burford, N.; Lumsden, M. D.; Decken, A. *Chem. Commun.* **2007**, 4668–4670.
(7) Godfrey, S. M.; Kelly, D. G.; McAuliffe, C. A.; Mackie, A. G.; Pritchard, R. G.; Watson, S. M. *J. Chem. Soc., Chem. Commun.* **1991**, 1163–1164.
(8) du Mont, W.-W.; Bätcher, M.; Pohl, S.; Saak, W. *Angew. Chem., Int. Ed. Engl.* **1987**, *26*, 912–913.
(9) du Mont, W.-W.; Stenzel, V.; Jeske, J.; Jones, P. G.; Sebald, A.; Pohl, S.; Saak, W.; Bätcher, M. *Inorg. Chem.* **1994**, *33*, 1502–1505.
(10) Stenzel, V.; Jeske, J.; du Mont, W.-W.; Jones, P. G. *Inorg. Chem.* **1997**, *36*, 443–448.
(11) Pohl, S. *Z. Anorg. Allg. Chem.* **1983**, *498*, 15–19.
(12) Pohl, S. *Z. Anorg. Allg. Chem.* **1983**, *498*, 20–24.
(13) du Mont, W.-W.; Kroth, H.-J. *J. Organomet. Chem.* **1976**, *113*, C35–C37.

Scheme 3. Halogenation Reaction of Diphosphines via a Phosphinophosphonium Cation

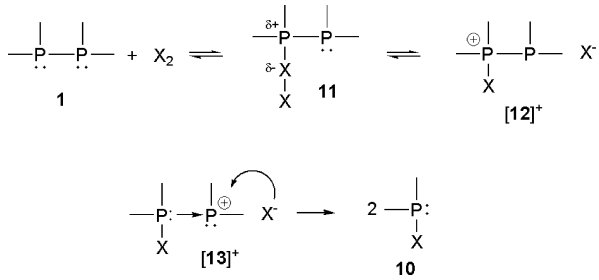

Scheme 4. Halogenation Reaction of *cyclo*-Polyphosphines[a]

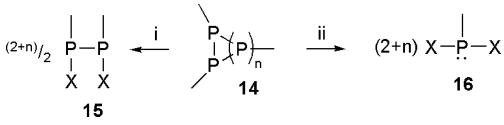

[a] (i) $^{(n+2)}/_2$ X_2; (ii) $(n+2)$ X_2 ($n = 1-4$).

Chart 1

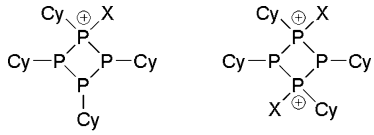

[17]$^+$ (X = I)
[19]$^+$ (X = Cl)

[18]$^{2+}$ (X = I)
[20]$^{2+}$ (X = Cl)

the intermediate dihalodiphosphine **15** has been obtained from the reaction of Ph_5P_5 with 2.5 equiv of I_2.[15]

Derivatives of the phosphino-halophosphonium cation [**12**]$^+$ have been previously isolated in conjunction with a weakly basic anion.[1,16−20] In this context, the formation of phosphino-halophosphonium cations as intermediates in the halogenation reaction of polyphosphine has been exploited as a synthetic approach to *catena*-phosphinophosphonium cations by sequestering the product halide X^- into a complex anion. This is demonstrated by the reactions of tetracyclohexyl-*cyclo*-tetraphosphine $(CyP)_4$ with $PhICl_2$, PCl_5 or I_2, in the presence of Me_3SiOTf or GaX_3 (X = Cl, I), which provide quantitative formation of salts containing the first *cyclo*-2-halo-1,3,4-triphosphino-2-phosphonium cations [**17**]$^+$ and [**19**]$^+$, and the first *cyclo*-2,4-dihalo-1,3-diphosphino-2,4-diphosphonium dication [**20**]$^{2+}$ (Chart 1). The new *cyclo*-phosphino-halophosphonium cation [**20**]$^{2+}$ can be considered as a phosphine−phosphenium donor−acceptor complex and undergoes ligand exchange reactions with PMe_3 or 1,2-bis(dimethylphosphino)ethane (dmpe) to effect dissociation of the homocyclic framework and forming phosphinodiphosphonium cations and diphosphinodiphosphonium dications.

Experimental Section

General Considerations. All reactions were carried out in a dry box under an inert N_2 atmosphere. Dichloromethane and pentane were dried on an MBraun solvent purification system, degassed with three freeze−pump−thaw cycles, and stored under nitrogen and over molecular sieves prior to use. Acetonitrile (sure seal), phosphorus pentachloride, gallium(III) chloride, gallium(III) iodide, trimethylsilyl trifluoromethansulfonate (Me_3SiOTf), and 1,2-bis-(dimethylphosphino)ethane (dmpe) were purchased from Sigma-Aldrich. Dichloroiodobenzene ($PhICl_2$) and tetracyclohexyltetraphosphinane (**2**) were prepared according to literature procedures.[21,22] All new compounds (unless otherwise stated) were characterized by $^{31}P\{^1H\}$, including measurement of ^{31}P (non-decoupled) and $^{31}P-^{31}P$ DQF COSY. Measurements were performed at 25 °C. Bruker AVANCE 500 (^{31}P (202.46 MHz)) and chemical shifts are referenced to $\delta_{H3PO4(85\%)} = 0.00$ and are reported in ppm; J values are reported in Hz. For compounds that give rise to higher order spin-systems in their $^{31}P\{^1H\}$ NMR spectra, the resolution-enhanced $^{31}P\{^1H\}$ spectra were transferred to the software program gNMR, version 5.0, by Cherwell Scientific.[23] After examining the line properties and noise, peak picking was performed. The full line-shape iteration procedure of gNMR was applied to obtain the best match of the fitted to the experimental spectra along with the assignment of all the peaks revealed in the resolution-enhanced spectra. The signs for the $^1J(^{31}P,^{31}P)$ coupling constants were set negative and all other signs were obtained accordingly.[24,25] Melting points were recorded on an electrochemical melting point apparatus in sealed capillary tubes under dinitrogen atmosphere and are uncorrected. Raman spectra were obtained for powdered and crystalline samples on a Bruker RFS 100 instrument equipped with a Nd:YAG laser (1064 nm). Chemical analyses were determined by Canadian Microanalytical Service LTD., Delta, BC, Canada.

Preparation of [17][GaI_4]·1/2 CH_2Cl_2. A solution of I_2 (5 mL, 0.05M, in CH_2Cl_2; 0.25 mmol) was added dropwise to a stirred solution of $(CyP)_4$ (114 mg, 0.25 mmol) and GaI_3 (113 mg, 0.25 mmol) in CH_2Cl_2 (8 mL). The reaction mixture was stirred at room temperature for 10 min, and the formation of the monocation was confirmed by ^{31}P NMR spectroscopy. The solvent was partially removed in vacuo (∼5 mL), and the solution was filtered and layered with pentane (5 mL) and stored at −32 °C. Pale-yellow crystals of [**17**][GaI_4]·1/2 CH_2Cl_2 were obtained after 4 days. Data for [**17**][GaI_4]·1/2 CH_2Cl_2: Yield: 42% (122 mg, 0.11 mmol); m.p. 118−120 °C; Raman (300 mW, 25 °C, cm^{-1}): 2968 (18), 2933 (100), 2889 (39), 2867 (40), 2846 (57), 1439 (24), 1343 (17), 1297 (18), 1266 (16), 1187 (16), 1103 (12), 1076 (12), 1025 (27), 997 (15), 848 (18), 814 (21), 737 (20), 506 (17), 479 (18), 465 (17), 427 (20), 398 (28), 363 (16), 328 (15), 267 (37), 214 (36), 189 (34), 167 (31), 145 (87), 123 (34); $^{31}P\{^1H\}$ NMR (CD_2Cl_2, 300 K, [ppm]): −44.2 (2P, $\boldsymbol{P}_A$), −31.1 (1P, $\boldsymbol{P}_M$), 34.8 (1P, $\boldsymbol{P}_X$, A_2MX spin system, $^1J_{AM} = -260$, $^1J_{MX} = -140$, $^2J_{AX} = -8$ Hz). Chemical analyses proved to be problematic for [**17**][GaI_4]·1/2 CH_2Cl_2 owing to the partial removal of solvents of crystallization upon isolation (Figure 1).

Reaction of 2 with $PhICl_2$ in the Presence of Me_3SiOTf. A solution of freshly prepared $PhICl_2$ [(i) 75 mg, 0.275 mmol, in 5 mL CH_2Cl_2; (ii) 137 mg, 0.5 mmol, in 5 mL CH_2Cl_2] was added

(14) Fild, M.; Hollenberg, I.; Glemser, O. *Naturwissenschaften* **1967**, *54*, 89–90.
(15) Hoffmann, H.; Grünwald, R. *Chem. Ber.* **1961**, *94*, 186–193. In this contribution, $(PhP)_5$ was misleadingly assigned as $(PhP)_4$.
(16) Burford, N.; Cameron, T. S.; LeBlanc, D. J.; Losier, P.; Sereda, S.; Wu, G. *Organometallics* **1997**, *16*, 4712–4717.
(17) Burford, N.; Ragogna, P. J. *Dalton Trans.* **2002**, 4307–4315.
(18) Burford, N.; Ragogna, P. J.; McDonald, R.; Ferguson, M. *J. Am. Chem. Soc.* **2003**, *125*, 14404–14410.
(19) Weigand, J. J.; Burford, N.; Lumsden, M. D.; Decken, A. *Angew. Chem., Int. Ed.* **2006**, *45*, 6733–6737.
(20) Weigand, J. J.; Burford, N.; Decken, A. *Eur. J. Inorg. Chem.* **2008**, 4343–4347.
(21) Krassowska-Świebocka, B.; Prokopenko, G.; Skulski, L. *Synlett* **1999**, *9*, 1409–1410.
(22) Henderson, Wm. A.; Epstein, M., Jr.; Seichter, F. S. *J. Am. Chem. Soc.* **1963**, *85*, 2462–2466.
(23) Budzelaar, P. H. M. *gNMR for Windows*, 5.0; Cherwell Scientific Publishing Limited: Oxford, UK, 1997.
(24) Finer, E. G.; Harris, R. K. *Prog. Nucl. Magn. Reson. Spectrosc.* **1970**, *6*, 61–118.
(25) Forgeron, M. A. M.; Gee, M.; Wasylishen, R. E. *J. Phys. Chem. A* **2004**, *108*, 4895–4908.

dropwise to a stirred solution of **2** (114 mg, 0.25 mmol) and Me_3SiOTf [(i) 45 μL, 0.25 mmol; (ii) 90 μL, 0.5 mmol] in CH_2Cl_2 (5 mL) at room temperature. The reaction was monitored by of $^{31}P\{^1H\}$ NMR spectroscopy (Figure 2, i and ii).

Preparation of [23][$GaCl_4$]. A solution of $GaCl_3$ (88 mg, 0.5 mmol, in 8 mL CH_2Cl_2) was added dropwise to a stirred solution of PCl_5 (104 mg, 0.5 mmol) in CH_2Cl_2 (10 mL). The reaction mixture was stirred at room temperature for 10 min and stored at −32 °C. Clear, colorless needles of [**23**][$GaCl_4$] started to separate after 1 day. Data for [**23**][$GaCl_4$]: Yield: 95% (182 mg, 0.48 mmol); m.p. 308−310 °C; Raman (280 mW, 25 °C, cm^{-1}): 650 (16, $\nu_3(F_2)$, PCl_4^+), 455 (100, $\nu_1(A_1)$, PCl_4^+), 373 (2, $\nu_3(F_2)$, $GaCl_4^-$), 347 (61, $\nu_1(A_1)$, $GaCl_4^-$), 250 (74, $\nu_4(F_2)$, PCl_4^+), 178 (34, $\nu_2(E)$, PCl_4^+), 151 (35, $\nu_4(F_2)$, $GaCl_4^-$), 121 (39, $\nu_2(E)$, $GaCl_4^-$); $^{31}P\{^1H\}$ NMR (CD_2Cl_2, 300 K, [ppm]): $\delta = 85.1$ (s).

Reaction of 2 with PCl_5 in the Presence of $GaCl_3$. A solution of freshly prepared PCl_5 (104 mg, 0.5 mmol, in 4 mL CH_2Cl_2) was added dropwise to a stirred solution of **2** (114 mg, 0.25 mmol) and $GaCl_3$ (176 mg, 1.0 mmol) in CH_2Cl_2 (5 mL) at room temperature. The reaction was monitored by $^{31}P\{^1H\}$ NMR spectroscopy (Figure 3).

Preparation of [19][$GaCl_4$] and [20][Ga_2Cl_7]$_2$. A solution of PCl_5 [(i) 52 mg, 0.25 mmol, in 5 mL CH_2Cl_2; (ii) 104 mg, 0.5 mmol, in 8 mL CH_2Cl_2] was added dropwise to a stirred solution of $(CyP)_4$ (114 mg, 0.25 mmol) and $GaCl_3$ [(i) 44 mg, 0.25 mmol; (ii) 176 mg, 1.0 mmol] in CH_2Cl_2 (8 mL). The reaction mixture was stirred at room temperature for 10 min, and the formation of (i) $[\mathbf{19}]^+$ or (ii) $[\mathbf{20}]^{2+}$ was confirmed by ^{31}P-NMR spectroscopy. The solvent was partially removed in vacuo (∼5 mL), and the solution was layered with pentane (5 mL) and stored at −32 °C. Colorless crystals of [**19**][$GaCl_4$] or [**20**][Ga_2Cl_7]$_2$ formed after a few days. Data for [**19**][$GaCl_4$]: Yield: 60% (106 mg, 0.15 mmol); m.p. 119−122 °C; Raman (300 mW, 25 °C, cm^{-1}): 2939 (100), 2890 (49), 2850 (80), 1495 (14), 1442 (32), 1344 (20), 1298 (19), 1267 (21), 1190 (16), 1080 (12), 1025 (26), 1000 (17), 849 (22), 816 (18), 734 (22), 572 (20), 461 (24), 423 (30), 367 (28), 344 (43), 291 (25), 166 (37), 150 (37), 121 (44); $^{31}P\{^1H\}$ NMR (CD_2Cl_2, 300 K, [ppm]): −54.4 (P, $\boldsymbol{P}_A$), −40.7 (2P, $\boldsymbol{P}_M$), 95.1 (1P, $\boldsymbol{P}_X$, AM_2X spin system, $^1J_{AM} = -285$, $^1J_{MX} = -126$, $^2J_{AX} = 18$ Hz); elemental analysis for $C_{24}H_{44}Cl_5GaP_4$ (703.49): calcd C 41.0, H 6.3; found: C 41.3, H 6.4. Data for [**20**][Ga_2Cl_7]$_2$: Yield: 90% (293 mg, 0.23 mmol); m.p. 106−109 °C; Raman (300 mW, 25 °C, cm^{-1}): 2944 (100), 2900 (360), 2859 (50), 1442 (18), 1342 (13), 1299 (9), 1290 (10), 1266 (12), 1192 (13), 1176 (12), 1106 (5), 1080 (7), 1022 (20), 993 (14), 843 (15), 800 (7), 743 (8), 720 (11), 592 (14), 471 (8), 420 (20), 369 (68), 357 (18), 287 (17), 262 (10), 234 (10), 212 (12), 191 (19), 166 (26), 138 (54); $^{31}P\{^1H\}$ NMR (CD_2Cl_2, 300 K, [ppm]): 9.3 (2P, $\boldsymbol{P}_A$), 83.2 (2P, $\boldsymbol{P}_X$, A_2X_2 spin system, $^1J_{AX} = -288$); elemental analysis for $C_{24}H_{44}Cl_{16}Ga_4P_4$ (1302.64): calcd C 22.1, H 3.4; found: C 22.1, H 3.6.

Preparation of [24][$GaCl_4$]. Method A: A solution of PCl_5 (104 mg, 0.50 mmol, in 8 mL CH_2Cl_2) was added dropwise to a stirred solution of [**20**][Ga_2Cl_7]$_2$ (130 mg, 0.10 mmol) in CH_2Cl_2 (4 mL). The reaction mixture was stirred at room temperature for 5 h. The solvent was partially removed in vacuo (∼5 mL), the solution was layered with pentane (5 mL) and stored at −32 °C. Method B: To solution of **2** (91 mg, 0.20 mmol) and $GaCl_3$ (144 mg, 0.80 mmol) in CH_2Cl_2 (5 mL) was slowly added a solution PCl_5 (332 mg, 1.60 mmol) in CH_2Cl_2 (6 mL) at room temperature. The solvent was partially removed in vacuo (∼5 mL), the solution was layered with pentane (5 mL) and stored at −32 °C. For both cases, colorless crystals of [**24**][$GaCl_4$] were formed within two days. Data for [**24**][$GaCl_4$]: Yield: 74% (160 mg, 0.37 mmol, method A); quantitative (method B); m.p. 96−98 °C; Raman (300 mW, 25 °C, cm^{-1}): 2959 (61), 2908 (25), 2872 (66), 2860 (65), 1515 (14), 1447 (48), 1351 (22), 1328 (17), 1296 (27), 1283 (20), 1268 (24), 1208 (17), 1179 (17), 1079 (17), 1027 (24), 1000 (21), 846 (22), 819 (27), 760 (24), 632 (29), 549 (52), 488 (55), 432 (41), 369 (31), 344 (100), 336 (83), 308 (44), 223 (54), 204 (61), 173 (37), 151 (55), 120 (84); $^{31}P\{^1H\}$ NMR (CD_2Cl_2, 300 K, [ppm]): $\delta = 127.2$ (s); elemental analysis for $C_6H_{11}Cl_7GaP$ (432.02): calcd C 16.7, H 2.6; found: C 16.5, H 2.6.

Preparation of [27][$GaCl_4$]. To a cooled solution (0 °C) of PMe_3 (0.52 M in toluene, 1 mL, 0.52 mmol) in CH_2Cl_2 (5 mL) was added a solution of [**20**][Ga_2Cl_7]$_2$ (169 mg, 0.13 mmol) in CH_2Cl_2 (2 mL) within 2 min. After 15 min the reaction mixture was allowed to warm to room temperature and stirred for a further 24 h. The oily phase was separated and dissolved in MeCN (1.5 mL). The MeCN solution was under-layered with CH_2Cl_2 and stored at −20 °C. After four days, [**27**][$GaCl_4$]$_2$ was obtained as block shaped crystals. Data for [**27**][$GaCl_4$]$_2$: Yield: 35% (73 mg); $^{31}P\{^1H\}$ NMR (CD_3CN, 300 K, [ppm]): only one diastereomer observed, broad signals, $\delta = -33.1$ (AA′) and 19.2 (XX′); elemental analysis for $C_{18}H_{40}Cl_8Ga_2P_4$ (803.48): calcd C 26.9, H 5.0; found: C 27.2, H 5.3.

Preparation of [29][$GaCl_4$]$_2$. A solution of dmpe (41.7 μL, 37.5 mg, 0.25 mmol) in CH_2Cl_2 (3 mL) was added dropwise within 30 min to a cooled (0 °C) solution of [**20**][Ga_2Cl_7]$_2$ (163 mg, 0.125 mmol) in CH_2Cl_2 (10 mL). After warming to room temperature, the formed precipitate was separated and washed with hexane (2 × 6 mL). The precipitate was dissolved in MeCN (3 mL), carefully under-layered with CH_2Cl_2 (5 mL), and stored at −20 °C. Colorless crystals of [**29**][$GaCl_4$]$_2$ were formed within three days. Data for [**29**][$GaCl_4$]$_2$: Yield: 85% (146 mg, 0.21 mmol); m.p. 146−148 °C; Raman (300 mW, 25 °C, cm^{-1}): 2990 (34), 2943 (48), 2924 (49), 2908 (100), 2859 (25), 1444 (20), 1395 (21), 1342 (16), 1300 (17), 1261 (18), 1192 (17), 1022 (18), 997 (17), 845 (19), 804 (20), 770 (21), 743 (22), 729 (23), 651 (33), 453 (34), 421 (33), 369 (−44), 348 (66), 320 (31), 247 (39), 218 (39), 179 (37), 149 (45), 120 (42); $^{31}P\{^1H\}$ NMR (CD_3CN, 300 K, [ppm]): −68.8 (1P, -P-$\boldsymbol{P}_A$-P-), 50.0 (2P, -$\boldsymbol{P}_X$-P-$\boldsymbol{P}_X$-, AX_2 spin system, $^1J_{AX} = -293$); elemental analysis for $C_{12}H_{27}Cl_8Ga_2P_3$ (687.33): calcd C 21.0, H 4.0; found: C 21.4, H 4.2.

Formation of a Mixture of [29][$GaCl_4$]$_2$ and [30][$GaCl_4$]$_2$. A solution of [**20**][Ga_2Cl_7]$_2$ (163 mg, 0.125 mmol) in CH_2Cl_2 (2 mL) was added all at once at room temperature to a solution of dmpe (41.7 μL, 37.5 mg, 0.25 mmol) in CH_2Cl_2 (3 mL). The immediate formation of an oil was observed. The oily phase was separated and dissolved in MeCN (3 mL), and the formed precipitate (Cy_4P_4) separated. To the clear solution was added CH_2Cl_2 (5 mL) and an approximate 1:1 mixture (as shown by $^{31}P\{^1H\}$ NMR) of compound [**29**][$GaCl_4$]$_2$ and [**30**][$GaCl_4$]$_2$ was obtained as a precipitate. Data for [**29**][$GaCl_4$]$_2$ and [**30**][$GaCl_4$]$_2$: Yield: 125 mg; $^{31}P\{^1H\}$ NMR (CH_3CN, C_6D_6 Capillary, 300 K, [ppm]); [**29**][$GaCl_4$]$_2$: $\delta = -68.8$ (1P, -P-$\boldsymbol{P}_A$-P-), 50.0 (2P, --$\boldsymbol{P}_X$-P-$\boldsymbol{P}_X$-, AX_2 spin system, $^1J_{AX} = -293$); [**30**][$GaCl_4$]$_2$: $\delta = -55.9$ (2P, -P-$\boldsymbol{P}_A$-$\boldsymbol{P}_A$-P-), 18.8 (2P, -$\boldsymbol{P}_X$-P-P-$\boldsymbol{P}_X$-, AA′XX′ spin system, $^1J_{AX} = {}^1J_{A'X'} = -315$, $^2J_{AA'} = 151$, $^2J_{AX'} = {}^2J_{XA'} = 18$, $^3J_{XX'} = -9$ Hz).

Crystal Structures. Suitable single crystals for all compounds were coated with Paratone-N oil, mounted using a glass fibre pin and frozen in the cold nitrogen stream of the goniometer. X-ray diffraction data for **2**[26] and [**29**][$GaCl_4$]$_2$ were collected on a Bruker AXS APEX CCD diffractometer equipped with a rotation anode at 153(2) K using graphite-monochromated Mo K_α radiation (λ = 0.71073 Å) with a scan width of 0.3° and 7 s for **2**, and 5 s for [**29**][$GaCl_4$]$_2$ exposure times. In both cases generator settings were 50 kV and 180 mA. Diffraction data were collected over the full sphere and were corrected for absorption. The data reduction (SAINT)[27] and correction (SADABS)[28] was performed with the Bruker software. X-ray diffraction data for [**17**][GaI_4]·1/2CH_2Cl_2, [**19**][$GaCl_4$], [**20**][Ga_2Cl_7]$_2$, [**23**][$GaCl_4$], [**24**][$GaCl_4$], and [**27**][$GaCl_4$]$_2$ were collected on a Rigaku RAXIS RAPID diffractometer with a imaging plate area detector (graphite-monochromated Mo K_α radiation, λ = 0.71073 Å). Crystals were mounted under fluorolube on the tip of 150 μm micromounts. The data were

(26) Henderson, W. A.; Epstein, M.; Seichter, F. S. *J. Am. Chem. Soc.* **1963**, *85*, 2462–2466.
(27) *SAINT 7.23A*; Bruker AXS, Inc: Madison, WI, 2006.
(28) Sheldrick, G. M. *SADABS*; Bruker AXS, Inc.: Madison, WI, 2004.

Table 1. Crystallographic Data

	2	[**17**][GaI_4]·1/2 CH_2Cl_2	[**19**][$GaCl_4$]	[**20**][Ga_2Cl_7]$_2$
formula	$C_{24}H_{44}P_4$	$C_{24.5}H_{45}ClP_4GaI_5$	$C_{24}H_{44}Cl_5P_4Ga$	$C_{24}H_{44}Cl_{16}P_4Ga_4$
M_r [g mol^{-1}]	456.47	1203.22	703.49	1302.63
dimension [mm^3]	0.16×0.13×0.13	0.27×0.19×0.16	0.29×0.27×0.21	0.27×0.14×0.06
color, habit	colorless block	yellow pinacoid	colorless block	colorless needle
crystal system	tetragonal	triclinic	monoclinic	orthorhombic
space group	$P\bar{4}2_1c$	$P\bar{1}$	$P2_1/n$	*P*bca
a [Å]	10.1235(2)	10.5502(3)	18.491(9)	17.8070(4)
b [Å]	10.1235(2)	13.5437(5)	9.143(9)	17.9537(3)
c [Å]	12.4110(5)	13.9971(5)	19.970(5)	31.5222(8)
α [deg]	90	101.395(2)	90	90
β [deg]	90	93.704(1)	104.27(5)	90
γ [deg]	90	99.350(2)	90	90
V [Å^3]	1271.94(6)	1924.9(1)	3272(5)	10077.7(4)
Z	2	2	4	8
T [K]	153(1)	123(2)	123(2)	123(2)
ρ_c [g cm^{-3}]	1.192	2.076	1.428	1.717
F(000)	496	1130	1456	5152
$\lambda_{MoK\alpha}$ [Å]	0.71073	0.71073	0.71073	0.71073
μ [mm^{-1}]	0.306	4.976	1.458	3.109
absorption correction	multi-scan	multi-scan	none	multi-scan
reflections collected	13577	96666	79803	86025
reflections unique	981	11152	6680	36726
R_{int}	0.0251	0.026	0.115	0.031
reflection obs. [$F > 3\sigma(F)$]	955	9830	5249	21819
residual density [e Å^{-3}]	0.249, −0.123	2.33, −1.74	1.12, −0.66	1.42, −0.79
parameters	65	472	352	477
GOF	1.112	1.077	1.000	0.970
R_1 [$I > 2\sigma(I)$]	0.0213	0.0258	0.0590	0.0478
wR_2 (all data)	0.0583	0.0305	0.0589	0.0593
CCDC	745539	745543	745537	745538

	[**23**][$GaCl_4$]	[**24**][$GaCl_4$]	[**27**][$GaCl_4$]$_2$	[**29**][$GaCl_4$]$_2$
formula	Cl_8GaP	$C_6H_{11}Cl_{17}GaP$	$C_{18}H_{40}Cl_8Ga_2P_4$	$C_{12}H_{27}Cl_8Ga_2P_3$
M_r [g mol^{-1}]	384.32	432.02	803.47	687.29
dimension [mm^3]	0.38×0.19×0.17	0.25×0.12×0.08	0.26×.25×0.22	0.14×.11×0.09
color, habit	colorless needle	colorless needle	colorless needle	colorless block
crystal system	orthorhombic	monoclinic	monoclinic	orthorhombic
space group	*P*bcm	$P2_1/c$	$P2_1/c$	$Pca2_1$
a [Å]	6.1146(3)	8.783(2)	9.740(2)	12.2913(3)
b [Å]	13.514(1)	13.740(3)	12.396(3)	14.9034(5)
c [Å]	13.792(1)	26.02(1)	28.660(7)	14.9881(6)
α [deg]	90	90	90	90
β [deg]	90	91.96(2)	90.19(1)	90
γ [deg]	90	90	90	90
V [Å^3]	1139.7(1)	3137(2)	3460.6(2)	2727.1(2)
Z	4	4	4	4
T [K]	123(2)	123(2)	123(2)	153(1)
ρ_c [g cm^{-3}]	2.240	1.829	1.542	1.674
F(000)	728	1696	1624	1368
$\lambda_{MoK\alpha}$ [Å]	0.71073	0.71073	0.71073	0.71073
μ [mm^{-1}]	4.361	3.015	2.368	2.935
absorption correction	multi-scan	multi-scan	multi-scan	multi-scan
reflections collected	8903	17765	48724	12814
reflections unique	1656	7802	7909	3810
R_{int}	0.030	0.040	0.101	0.0328
reflection obs. [$F > 3\sigma(F)$]	1397	6005	6752	3512
residual density [e Å^{-3}]	0.72, −0.97	1.22, −0.78	1.75, −1.29	0.634, −0.533
parameters	52	294	290	231
GOF	1.098	1.114	1.089	1.026
R_1 [$I > 3\sigma(I)$]	0.0338	0.0386	0.0662	0.0259
wR_2 (all data)	0.0376	0.0427	0.1876	0.0579
CCDC	745544	745541	745540	745542

collected using sweeps of ω oscillations. After data reduction, equivalent reflections were merged. Intensity data were corrected for Lorentz, absorption and polarization effects. For further crystal and data collection details, see Table 1. The structures were solved by direct methods and expanded Fourier techniques. Full matrix least-squares refinement was carried out with the program SHELXS97[29] against F^2 using first isotropic and later anisotropic thermal parameters for all non-hydrogen atoms. Hydrogen atoms were generated with idealized geometries and isotropically refined

(29) Sheldrick, G. M. *SHELXL-97, Program for crystal structure determination*; University of Göttingen: Germany, 1997.

Scheme 5. Preparation of [**17**][GaI_4] and Attempted Preparation of [**18**][GaI_4]$_2$ (X = GaI_4, OTf) Salts[a]

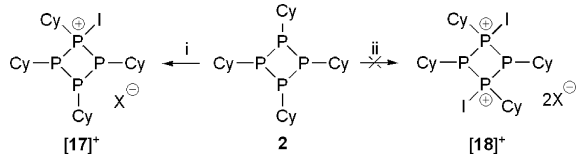

[a] (i) I_2, GaI_3, or AgOTf in CH_2Cl_2; (ii) $2I_2$, $2GaI_3$, or 2AgOTf in CH_2Cl_2.

Table 2. $^{31}P\{^1H\}$ NMR Parameters for Salts of Cations [**17**]$^+$, [**19**]$^+$, [**20**]$^{2+}$, [**27**]$^{2+}$, [**29**]$^{2+}$, and [**30**]$^{2+}$

	[**17**]$^+$	[**19**]$^+$	[**20**]$^{2+}$	[**27**]$^{2+}$	[**29**]$^{2+}$	[**30**]$^{2+}$
spin system[a,b]	A_2MX	AM_2X	A_2X_2	AA′XX′	AX_2	AA′XX′
δ_A[c]	−44.2	−54.4	9.3	−33.1	−68.8	−55.9
δ_M	−31.1	−40.7				
δ_X	34.8	95.1	83.2	19.2	50.0	18.8
$^1J_{AM}$[d]	−260	−285				
$^1J_{MX}$	−140	−126				
$^2J_{AX}$	−8	18				
$^1J_{AX}$, $^1J_{AA'}$			−288	−[e]	−293	−315, −151
$^2J_{A'X}$, $^3J_{XX'}$				−[e]		18, −9

[a] Furthest downfield resonance is denoted by the highest letter in the alphabet, and the furthest upfield by the lowest letter. By convention the letter in the spin system is determined by the ratio $\Delta\delta(P_iP_{ii})/J_{P_iP_{ii}} > 10$ (resonance considered to be pseudo-first order and the assigned letters are separated) < 10 (consecutive letters are assigned). [b] Parameters for spin systems of higher order are derived by iterative fitting of experimental data at 300 K. [c] Absolute signs of the $^1J_{PP(iso)}$ have been tentatively assigned to be negative. [d] Chemical shifts (δ) are given in [ppm] and coupling constants (J) in [Hz]. [e] Could not be simulated due to broad signals.

using a riding model. For [**27**][$GaCl_4$]$_2$ the crystal was a twin (twin law 1 0 0, 0 −1 0, 0 0 −1) with not quite equal components (0.509: 0.491). For compounds [**17**][GaI_4]·1/2CH_2Cl_2, [**19**][$GaCl_4$], [**20**][Ga_2Cl_7]$_2$, [**23**][$GaCl_4$], [**24**][$GaCl_4$], and [**27**][$GaCl_4$]$_2$ the calculations were performed using the CrystalStructure crystallographic software package.[30,31]

Results and Discussion

The halonium addition reaction that occurs when a phosphine reacts with a dihalogen has been extrapolated to polyphosphines to provide a new synthetic approach to phosphinophosphonium cations. The $^{31}P\{^1H\}$ NMR spectra of reaction mixtures containing $(CyP)_4$ (**2**), I_2 and GaI_3 in CH_2Cl_2 solution (Scheme 5) show three resonances in a first order A_2MX spin pattern with relative intensities of 2:1:1. The data are summarized in Table 2 and are consistent with the formation of the monocation [**17**]$^+$ (Chart 1). Chemical shifts at higher field correspond to the phosphine centers ($\delta_A = -44.2$ and $\delta_M = -31.1$ ppm) and the low field shift ($\delta_A = 34.8$ ppm) corresponds to the phosphonium center, in accordance with those for previously reported phosphinophosphonium cations.[1,17,32] Compound [**17**][GaI_4] was isolated as extremely air- and moisture-sensitive yellow blocks in moderate yields (42 %) as a CH_2Cl_2 solvate.

The solid state structure of [**17**]GaI_4·1/2 CH_2Cl_2 has been determined by X-ray crystallography and a view of the cation and anion in the solid state is shown in Figure 1. Selected

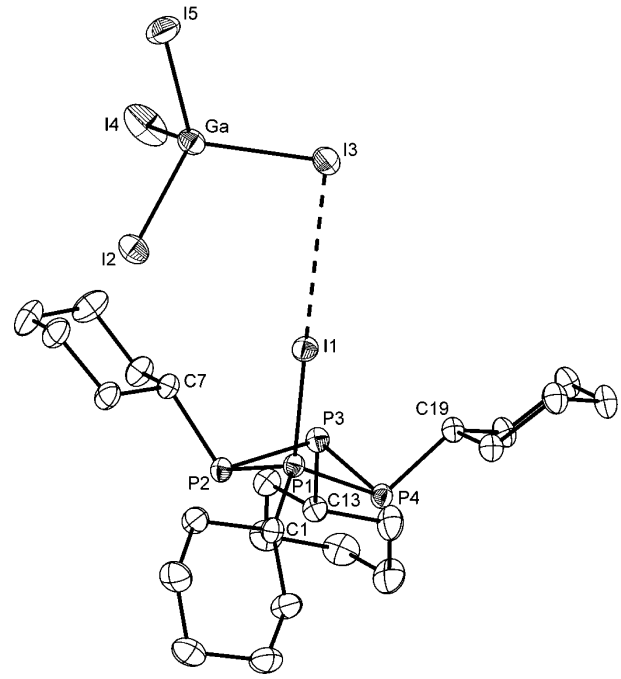

Figure 1. ORTEP plot of the molecular structure of the cation and anion in [**17**][$GaCl_4$]•1/2CH_2Cl_2. Thermal ellipsoids with 50% probability (hydrogen atoms and solvent molecules are omitted for clarity). Selected bond lengths (Å) and angles (°) are included in Table 2.

Table 3. Selected Structural Parameters for **2** and Cations [**17**]$^+$, [**19**]$^+$, and [**20**]$^{2+}$

	2	[**17**]$^+$ (X = I)	[**19**]$^+$ (X = Cl)	[**20**]$^{2+}$ (X = Cl)
		Bond Lengths [Å]		
P1−P2[a]	2.2224(5)	2.1872(8)	2.185(1)	2.1999(8)
P2−P3		2.2386(7)	2.2411(8)	2.2004(8)
P3−P4		2.2400(7)	2.2478(9)	2.2077(8)
P4−P1[a]	2.2224(5)	2.1919(8)	2.1857(8)	2.2084(8)
P1−X		2.4041(5)	2.011(1)	1.9828(9)
P3−X				1.9832(8)
P1−C1	1.868(1)	1.838(2)	1.814(2)	1.820(2)
P2−C7		1.864(2)	1.864(2)	1.865(2)
P3−C13		1.872(2)	1.873(2)	1.791(2)
P4−C19		1.863(2)	1.863(2)	1.867(2)
		Bond Angles [deg]		
P1−P2−P3[a]	85.271(9)	84.03(2)	83.71(3)	80.55(2)
P2−P3−P4		86.97(2)	88.71(3)	94.60(3)
P3−P4−P1		83.89(2)	83.52(3)	80.21(2)
P4−P1−P2		89.46(3)	91.79(3)	94.59(3)
P2−P1−C1	102.55(5)	113.29(7)	115.3(1)	110.83(8)
P4−P1−C1		115.26(7)	115.32(8)	114.21(8)
P1−P2−C7	102.81(5)	105.78(7)	103.97(9)	105.15(8)
P1−P4−C19		104.73(8)	105.51(8)	106.27(9)
P2−P3−C13		100.70(7)	98.37(8)	111.47(8)
P4−P3−C13		100.86(7)	100.35(9)	112.68(8)
P2−P1−X		113.79(2)	113.74(4)	113.34(3)
P4−P1−X		114.57(2)	113.46(3)	112.41(3)
P2−P3−X				113.96(3)
P4−P3−X				112.91(3)
C1−P1−X		113.79(2)	107.44(9)	110.64(9)
C13−P3−X				110.45(9)

[a] For **2** P1 = P3, P2 = P^i, P4 = P^{ii}, symmetry code: (i) $y - 1, -x + 1, -z + 2$; (ii) $-y + 1, x + 1, -z + 2$.

structural parameters are listed in Table 3 along with comparative parameters for the *cyclo*-tetraphosphine **2**. Consistent with the structural features of $[MeCy_4P_4]^+$,[4] the cyclohexyl substituent at P1 in [**17**]$^+$ minimizes the steric interactions by twisting to enable a *gauche* conformation of the α-hydrogen atom of C1 and the iodine substituent.[4] The P−P bonds at the four-

(30) CrystalStructure 3.8: Crystal Structure Analysis Package, Rigaku and Rigaku/MSC (2000−2006). 9009 New Trails Dr. The Woodlands TX 77381 USA.
(31) *CRYSTALS*, Issue 11; Carruthers, J. R., Rollett, J. S., Betteridge, P. W., Kinna, D., Pearce, L., Larsen, A., Gabe, E., Eds.; Chemical Crystallography Laboratory, Oxford, UK, 1999.
(32) Burford, N.; Ragogna, Cameron, T. S.; Ragogna, P. *J. Am. Chem. Soc.* **2001**, *123*, 7947–7948.

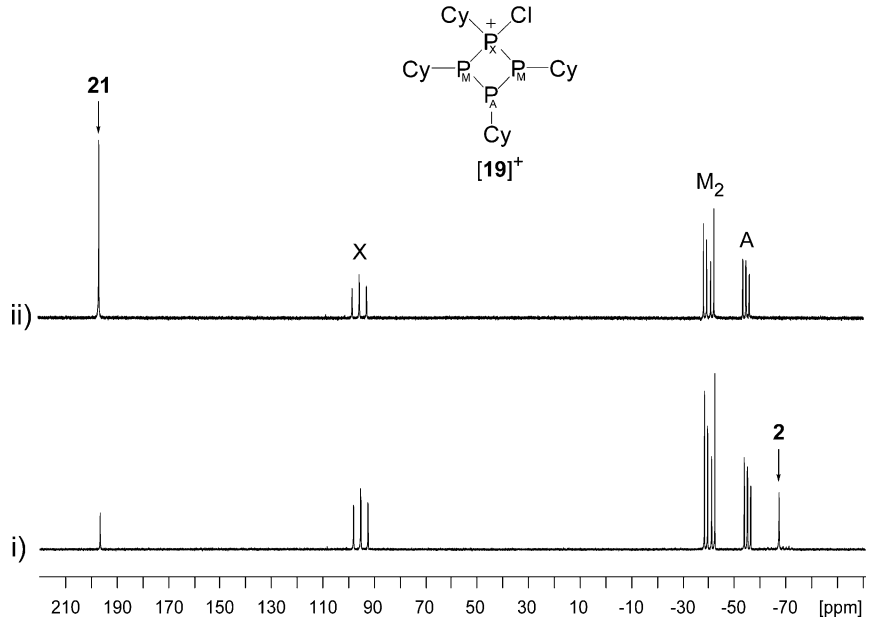

Figure 2. $^{31}P\{^1H\}$ NMR spectra of the reaction of $(CyP)_4$ with $PhICl_2$ in the presence of Me_3SiOTf at RT in CH_2Cl_2; (i) ~1.1 equiv of $PhICl_2$; (ii) 2 equiv of $PhICl_2$.

coordinate phosphorus centers are slightly shorter than those involving the three-coordinate phosphorus centers. Moreover, the shortest P−C bond occurs at the phosphonium center. The P_4 ring is slightly more puckered than that in $[MeCy_4P_4]^+$, as indicated by greater P−P−P−P torsion angles ranging from 23.6−24.2° (vs. 28.9−29.6°). The iodine atom at the phosphonium center has a weak interaction with an iodine of the gallate anion (3.635(3) Å), resulting in an almost linear P1−I1−I3 unit (168.37(2)°). The P−I bond length (2.4041(5) Å) is typical (2.40 ± 0.01 Å),[11,12,33] indicating that [**17**]GaI_4 should be considered as an ionic compound. Attempts to prepare the dication $[\mathbf{18}]^{2+}$, by treatment of **2** with 2 equiv of I_2 and GaI_3 or AgOTf, leads to the formation of copious amounts of an orange precipitate, found to be completely insoluble in CH_2Cl_2, CH_3CN, and C_6H_5F (Scheme 5). We abstained from a detailed investigation of the precipitate.

$^{31}P\{^1H\}$ NMR spectra of reaction mixtures containing $(CyP)_4$ (**2**), $PhICl_2$ and Me_3SiOTf in CH_2Cl_2 are summarized in Figure 2. Reaction mixtures involving an slight excess (1.1 equiv) of $PhICl_2$ exhibit an AM_2X spin system that is assigned to $[\mathbf{19}]^+$ (Table 2). The presence of $(CyP)_4$ ($\delta = -67.0$ ppm)[34] and $CyPCl_2$ (**21**, $\delta = -192.0$ ppm)[35] in this reaction mixture is significant as the $^{31}P\{^1H\}$ NMR spectrum of a reaction of **2** with 2 equiv of $PhICl_2$ in the presence of 2 equiv of Me_3SiOTf (Figure 2(ii)) shows only the presence of $[\mathbf{19}]^+$ and $CyPCl_2$ (**21**). We interpret these observations according to Scheme 6, which shows the initial chloronium addition to **2** to give $[\mathbf{19}]^+$ followed by a second addition to give the dication $[\mathbf{20}]^{2+}$. The dication is not observed implying fast nucleophilic attacks by Cl^- at the phosphonium centers to first displace cation $[\mathbf{22}]^+$ and **21**. Under these reaction conditions, we speculate that cation $[\mathbf{22}]^+$ undergoes a further and rapid[36] nucleophilic attack by Cl^- to give **21** and [CyP═PCy],[37] which dimerizes to give **2**. The characteristic A_2B pattern corresponding to $(CyP)_3$[38] was not observed in the chlorination reactions in contrast to the ring contraction of $[MeCy_4P_4]^+$, which is observed on reaction with PMe_3 to yield $(CyP)_3$ and the phosphinophosphonium cation $[Me_3P{-}PMeCy]^+$.[4]

Scheme 6. Proposed Pathway for Reaction of **2** with $PhICl_2$ in the Presence of Me_3SiOTf

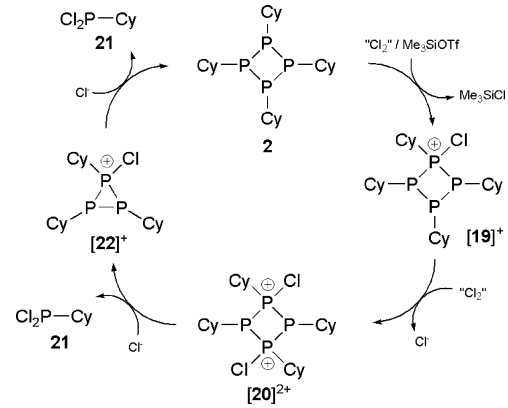

Chloronium addition to $(CyP)_4$ is also effected by reaction with PCl_5 and $GaCl_3$ in CH_2Cl_2. Reaction mixtures of various stoichiometries have been monitored by $^{31}P\{^1H\}$ NMR spectroscopy at room temperature as summarized in Figure 3. In the absence of PCl_5 (Figure 3, X = 0 equiv), the two broad signals ($\delta = -43$ and -62 ppm) are indicative of a weak adduct between $(CyP)_4$ and $GaCl_3$ which dissociates in solution. Introduction of a solution of PCl_5 in CH_2Cl_2 results in the formation of the tetrachlorophosphonium salt [**23**][$GaCl_4$], as shown in Scheme 7a, which reacts with $(CyP)_4$ to give $[\mathbf{19}]^+$ (AM_2X spin system, Table 2) and PCl_3 ($\delta = -220.1$ ppm; X

(33) Cotton, F. A.; Kibala, P. A. *J. Am. Chem. Soc.* **1987**, *109*, 3308–3312.
(34) Albrand, J. P.; Cogne, A.; Robert, J. B. *J. Am. Chem. Soc.* **1978**, *100*, 2600–2604.
(35) Weferling, N. *Z. Anorg. Allg. Chem.* **1987**, *548*, 55–62.
(36) Schoeller, W. W.; Staemmler, V.; Rademacher, P.; Niecke, E. *Inorg. Chem.* **1986**, *25*, 4382–4385.
(37) Diphosphenes (RP═PR) need bulky substituents for kinetic stabilization:Yoshifuji, M.; Shima, I.; Inamoto, K.; Hirotsu, K.; Higushi, T. *J. Am. Chem. Soc.* **1981**, *103*, 4587–4589.
(38) Baudler, M.; Pinner, C.; Gruner, C.; Hellmann, J.; Schwamborn, M.; Kloth, B. *Z. Naturforsch. B* **1977**, *32*, 1244–1251.

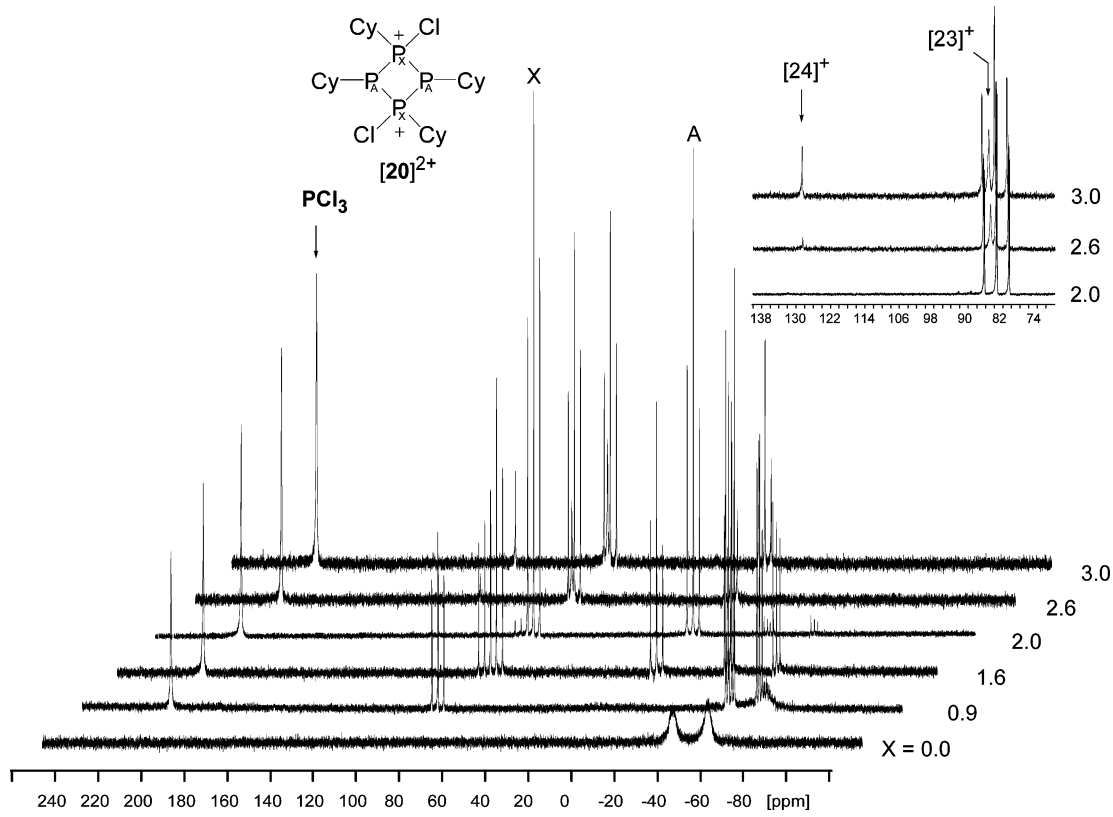

Figure 3. $^{31}P\{^1H\}$ NMR spectra (CH_2Cl_2, C_6D_6 capillary, RT) of the stepwise chlorination reaction of **2** with PCl_5 in the presence of $GaCl_3$ according to Scheme 7; X = 0−3 equiv of PCl_5.

Scheme 7. Successive Chlorination of $(CyP)_4$ with $[PCl_4]^+$

a) $PCl_5 + GaCl_4 \longrightarrow [PCl_4][GaCl_4]$
[23][GaCl4]

b) **2** + x[PCl4]+ [23]+ → x = 1: [19]+ + PCl3; x = 2: [20]2+ + 2PCl3

c) $(CyP)_4 + 4GaCl_4 + 8PCl_5 \longrightarrow [CyPCl_3][GaCl_4] + 8PCl_3$
[24][GaCl4]

= 1 equiv).[39] A high concentration of PCl_5 and $GaCl_3$ in solution leads to the crystallisation of [**23**][$GaCl_4$] as colorless needles.

The binary tetrachlorophosphonium cation [**23**]$^+$ has been known for some time and was characterized by vibrational[40] and ^{31}P NMR[41] spectroscopic studies, as well as by crystal structure determinations with a large combination of several counter-anions.[42] However, to the best of our knowledge, an X-ray determination of [**23**]$^+$ as the tetrachlorogallate salt has not been reported. Compound [**23**][$GaCl_4$] crystallizes in the orthorhombic space group *P*bca with four molecular units in the unit cell (Figure 4). The structure is isotypical with [PCl_4][$FeCl_4$].[43] The cation displays an almost perfect tetrahedral

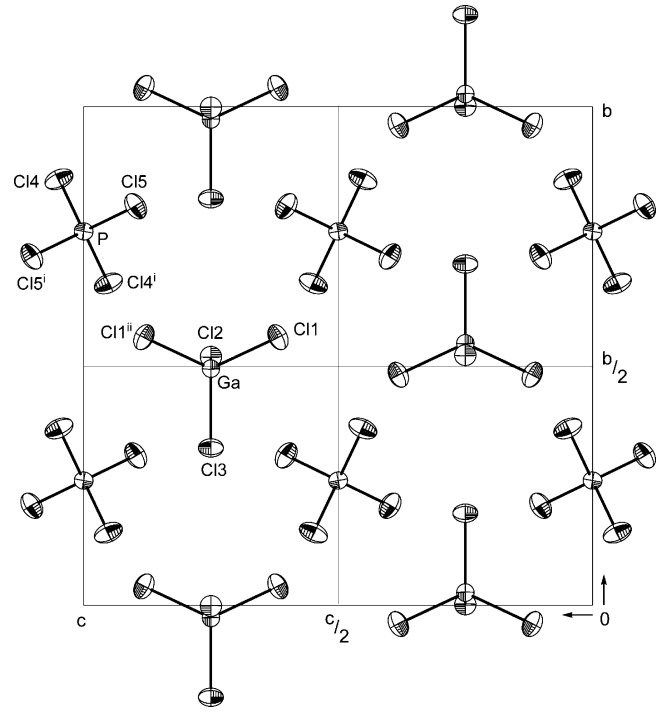

Figure 4. ORTEP plot of the perspective view of the unit cell of [**23**][$GaCl_4$] perpendicular to the *bc* plane. Thermal ellipsoids with 50% probability at 123(2) K [symmetry code: (i) *x*, 0.5 − *y*, −*z*; (ii) *x*, *y*, 0.5 − *z*].

geometry, whereas the anion is significantly distorted, exhibiting Cl−E−Cl angles between 108.69(2) and 113.47(2)° ([$GaCl_4$]$^-$) and between 108.43(5) and 110.38(3)° ([PCl_4]$^+$). This trend is

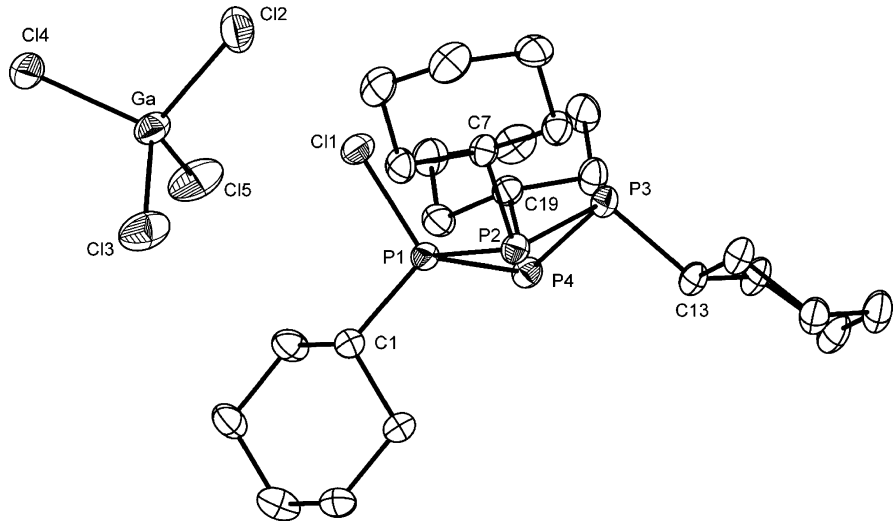

Figure 5. ORTEP plot of the molecular structure of [**19**][$GaCl_4$]. Thermal ellipsoids with 50% probability at 123(2) K (hydrogen atoms are omitted for clarity). Selected bond lengths (Å) and angles (deg) are included in Table 2.

also reflected by the Ga−Cl distances varying from 2.1704(7) to 2.1867(9)Å, whereas the P−Cl bond lengths are within the limits and are almost identical (1.9285(8) and 1.9302(9) Å). The molecular structure of [**23**][$GaCl_4$] shows short interatomic Cl···Cl distances in the range of 3.338(2) to 3.470(2) Å between the $[PCl_4]^+$ and $[GaCl_4]^-$ units, which are shorter than the sum of the van der Waals radii (3.50 Å),[44] indicating weak cation···anion interactions.

Two triplets, assigned to $[\mathbf{20}]^{2+}$, are observed when the stoichiometry of PCl_4^+ exceeds that of $(CyP)_4$ (Table 2; Scheme 7b, Figure 3, X = 2 equiv). The cations $[\mathbf{19}]^+$ and $[\mathbf{20}]^{2+}$ are resilient in this reaction mixture due to the absence of chloride anion. Addition of excess PCl_5 leads to appearance of two singlets attributed to $[\mathbf{23}]^{+41}$ (δ = 85.1ppm) and $[\mathbf{24}]^+$ (δ = 127.2 ppm). Cation $[\mathbf{24}]^+$ represents the final chlorination product of **2** when 8 equiv of PCl_5 are added (Scheme 7c). Equimolar reaction mixtures of $(CyP)_4$, $GaCl_3$, and PCl_3 in CH_2Cl_2 at room temperature have enabled isolation of [**19**][$GaCl_4$]. Similarly, [**20**][Ga_2Cl_7]$_2$ has been isolated from the 1:4:2 reaction of $(CyP)_4$, $GaCl_3$, and PCl_3 in CH_2Cl_2 (Scheme 7b). Both compounds were obtained as colorless needles. A view of the molecular units of [**19**][$GaCl_4$] and [**20**][Ga_2Cl_7]$_2$ is shown in Figures 5 and 6, respectively, and structural parameters are listed in Table 3.

The structural features of [**19**][$GaCl_4$] are comparable with those discussed for [**17**]GaI_4·1/2 CH_2Cl_2. The solid state structure of [**20**][Ga_2Cl_7]$_2$ contains a symmetric (approximate C_{2v}) cation $[\mathbf{20}]^{2+}$ consistent with the A_2X_2 spin system observed in the solution $^{31}P\{^1H\}$ NMR spectrum. The P−P bond lengths in $[\mathbf{20}]^{2+}$ are essentially identical [2.1999(8) to 2.2084(8) Å]

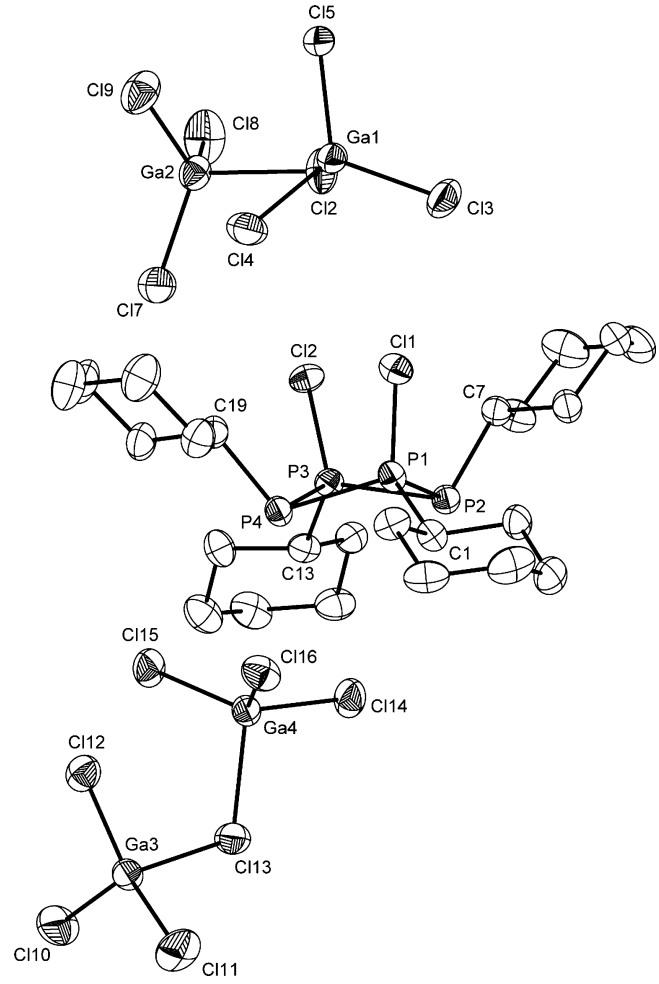

Figure 6. ORTEP plot of the molecular structure of [**20**][$GaCl_4$]. Thermal ellipsoids with 50% probability at 123(2) K (hydrogen atoms are omitted for clarity). Selected bond lengths (Å) and angles (deg) are included in Table 2.

and are only slightly shorter than those in $(CyP)_4$ [2.2224(5) Å] and in $[\mathbf{19}]^+$ [2.1872(8) to 2.2478(9) Å]. The P−Cl bonds [1.9828(9) and 1.9832(8) Å] in $[\mathbf{20}]^{2+}$ are shorter than that in $[\mathbf{19}]^+$ [2.011(1) Å] as expected due to the higher charge in the

(39) Johnson, S. E.; Knobler, C. B. *Phosphorus, Sulfur and Silicon* **1996**, *115*, 227–240.
(40) (a) Shamir, J.; van der Veken, B. J.; Herman, M. A.; Rafaeloff, R. *J. Raman Spectrosc.* **1981**, *11*, 215–220. (b) Finch, A.; Gates, P. N.; Muir, A. S. *Polyhedron* **1986**, *5*, 1537–1542.
(41) Dillon, K. B.; Nisbet, M. P.; Waddington, T. C. *J. Chem. Soc., Dalton Trans.* **1978**, *11*, 1455–1460.
(42) Aubauer, C.; Kaupp, M.; Klapötke, T. M.; Nöth, H.; Piotrowski, H.; Schnick, W.; Senker, J.; Suter, M. *J. Chem. Soc., Dalton Trans.* **2001**, 1880–1889, and references therein.
(43) Kistenmacher, T. J.; Stucky, G. D. *Inorg. Chem.* **1968**, *10*, 2150–2155.
(44) Bondi, A. *J. Phys. Chem.* **1964**, *68*, 441–451.

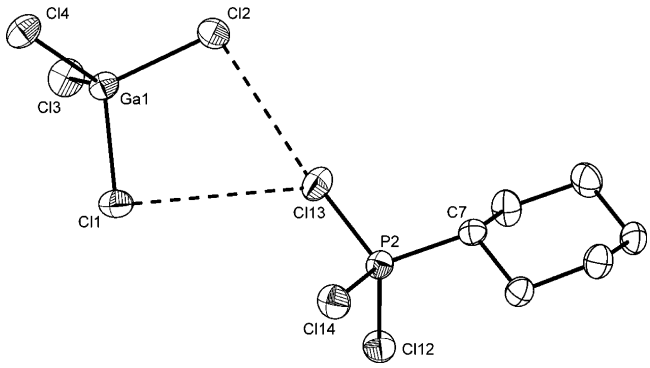

Figure 7. ORTEP plot of [**24**][$GaCl_4$]$_2$. Thermal ellipsoids with 50% probability (hydrogen atoms and counteranions are omitted for clarity) Only one cation of the asymmetric unit and the interaction of the counteranion is shown. Selected bond lengths (Å) and angles (deg): P2−Cl12 1.954(1), P2−Cl13 1.953(1), P2−Cl14 1.954(1), P2−C7 1.792(2), Ga1−Cl1 2.1834(7), Ga1−C2 2.1932(8), Ga1−Cl3 2.1753(8), Ga1−Cl4 2.1578(8), Cl12−P2−Cl13 108.36(4), Cl12− P2−Cl14 107.94(5), Cl12−P2−C7 110.57(9), Cl13−P2−Cl14 107.66(4), Cl13−P2−C7 110.7(1), Cl14−P2−C7 111.52(9).

Scheme 8. Formation of *acyclic*-2,3-Diphosphino-1,4-diphosphonium Dication [**27**]$^{2+}$ via Displacement Reaction of [**20**]$^{2+}$ with PMe_3 and Proposed Mechanism

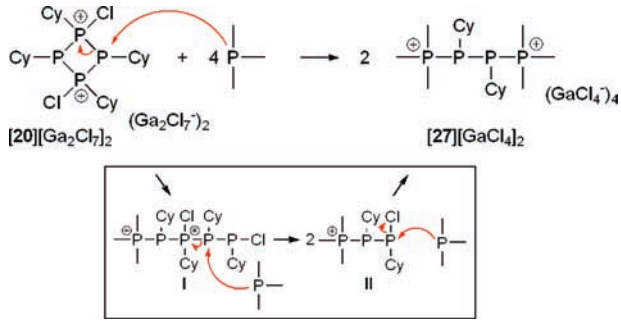

dication. The P−C bond lengths at the phosphonium centers in [**19**]$^+$ and [**20**]$^{2+}$ [1.791(2) to 1.820(2) Å] are significantly shorter than those at the phosphine centers [1.863(2) to 1.873(2) Å]. The $[GaCl_4]^-$ anions in [**19**][$GaCl_4$] adopt a slightly distorted tetrahedral geometry with Cl−Ga−Cl bond angles between 107.36(3) and 111.94(4)°. The anion in [**20**][Ga_2Cl_7]$_2$, which is isosteric with Cl_2O_7,[45] contains two distorted tetrahedral gallium centers associated via a chloride bridge with a mean Ga−Cl−Ga bond angle of 110.88(4)°. The *gauche* conformation of the $[Ga_2Cl_7]^-$ anion can be explained by the minimization of Cl−Cl interactions.[46] The molecular structures of [**19**][$GaCl_4$] and [**20**][Ga_2Cl_7]$_2$ show no interion Cl···Cl interactions.

In the presence of excess PCl_5 and $GaCl_3$ in CH_2Cl_2, $(CyP)_4$ dissociates to give [**24**][$GaCl_4$] quantitatively (Scheme 7c), which crystallizes with two independent, but essentially identical formula units of [**24**][Ga_2Cl_7]$_2$ in the unit cell. A view of one of the molecular units is depicted in Figure 7. The mean P−Cl bond lengths (1.954 Å) in the cations are slightly shorter than those in the monocation [**19**]$^+$ (2.011(1) Å) and the dication [**20**]$^{2+}$ (1.983(1) Å) due to the inductive effect of the chloro substituents in [**24**]$^+$. The Cl−P−Cl and Cl−P−C angles range from 107.86(4) to 111.60(9)° consistent with the tetrahedral arrangement of the cation. The Cl···Cl contact (3.281(2) Å)

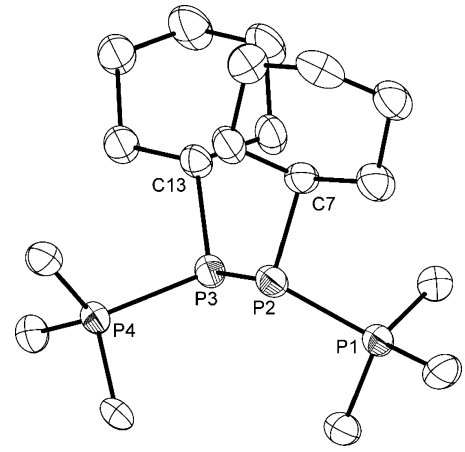

Figure 8. ORTEP plot of the molecular structure of the cation [**27**]$^{2+}$ in [**27**][$GaCl_4$]$_2$. Thermal ellipsoids with 50% probability (hydrogen atoms and counteranions are omitted for clarity). Selected bond lengths (Å), angles (deg) and dihedral angles: P1−P2 2.186(2), P2−P3 2.227(2), P3−P4 2.198(2), P2−C7 1.874(6), P2−C7 1.879(5); P1−P2−P3 94.98(8), P2−P3−P4 95.10(8), P1−P2−C7 107.6(2), P3−P2−C7 107.9(2), P2−P3−C13 107.1(2), P4−P3−C13 107.3(2), Cl12−P2−C7 110.57(9), Cl13−P2−Cl14 107.66(4), Cl13−P2−C7 110.7(1), Cl14−P2−C7 111.52(9); P1−P2−P3−P4 132.13(8), C7−P2−P3−C13 −7.6(2), C7−P2−P3−P4− 117.5(2), C13−P3−P2−P1 −118.0(2).

between Cl13 of [**24**]$^+$ and Cl2 of $[GaCl_4]^-$ is within the sum of the van der Waals radii (r_{Cl} = 1.75 Å, $2r_{Cl}$ = 3.50 Å),[44] classifying this as a weak donor−acceptor interaction.

The $^{31}P\{^1H\}$ NMR spectra of the slow addition of 1 equiv [**20**][Ga_2Cl_7]$_2$ to 4 equiv of PMe_3 show mainly two broad signals ($\delta_A = -33.1$, $\delta_X = 19.2$ ppm; Table 2) due to fluxional behavior that in accordance to other observation are assigned to the 2,3-diphosphino-1,4-diphosphonium dication [**27**]$^{2+}$ (Scheme 8). As shown in Scheme 8, nucleophilic attack of dication [**20**]$^{2+}$ by PMe_3 is proposed to give the five-membered monocation **I**, which is subsequently attacked by a second equivalent PMe_3 to yield monocation **II**.[47] The $^{31}P\{^1H\}$ NMR spectrum of a test reaction obtained from the slow addition of 2 equiv PMe_3 to dication [**27**]$^{2+}$ is complicated, however, an AMX spin system with resonances at −40.5 ($1P_A$, dd, $^1J_{AM}$ = 293, $^1J_{AX}$ = 312 Hz), 17.3 ($1P_M$, dd, $^1J_{AM}$ = 293, $^2J_{MX}$ = 47 Hz), and 95.7 ($1P_X$, dd, $^1J_{AX}$ = 312, $^2J_{MX}$ = 47 Hz) ppm indicates the formation of cation $[Me_3P_MP_ACyP_XCyCl]^+$ (**II**) as an intermediate. We envisage that cation **II** subsequently undergoes conversion to dication [**20**]$^{2+}$ with addition of PMe_3. Colorless crystals of [**27**][$GaCl_4$]$_2$ were obtained in low yield (35%), but spectroscopic characterization was hampered by dynamic behavior in solution. The solid state structure of the cation [**27**]$^{2+}$ (Figure 8) is consistent with those of other derivatives[48,49,47] prepared by reductive coupling of chlorophosphinophosphonium ions [**12**]$^+$ (Scheme 9), and the eclipsed conformation of the central C−P−P−C framework [torsion angle of 7.7(3)°] is due to a combination of steric interactions in the terminal and internal positions.[47]

The reaction of [**20**][Ga_2Cl_7]$_2$ with PMe_3 can be considered as a ligand-induced cyclodissociation, highlighting [**27**]$^{2+}$ as a

(45) Simon, A.; Borrmann, H. *Angew. Chem., Int. Ed.* **1981**, *27*, 1339–1341.
(46) Meyer, G.; Blachnik, R. *Anorg. Allg. Chem.* **1983**, *503*, 126–132.
(47) Carpenter, Y.-Y.; Dyker, C. A.; Burford, N.; Lumsden, M. D.; Decken, A. *J. Am. Chem. Soc.* **2008**, *130*, 15732–15741.
(48) Karaghiosoff, K. Ph.D. Thesis, Ludwig-Maximilians-Universität: Munich, Germany, 1986.
(49) Dyker, C. A.; Burford, N.; Lumsden, M. D.; Decken, A. *J. Am. Chem. Soc.* **2006**, *128*, 9632–9633.

Scheme 9. Formation of *acyclic*-2,3-Diphosphino-1,4-diphosphonium Dications $[\mathbf{25}]^{2+}$ via Reductive Coupling Reactions of a Chlorophosphoniumphosphine ($[\mathbf{12}]^{+}$) with Phosphines[47]

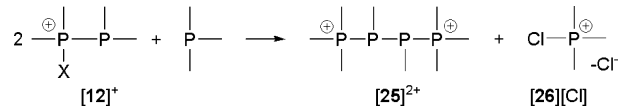

Scheme 10. Formation of *cyclic*-2,3-Diphosphino-1,4-diphosphonium Dications $[\mathbf{28}]^{2+}$ via Reductive Coupling Reaction According to Dillon and Co-workers[50]

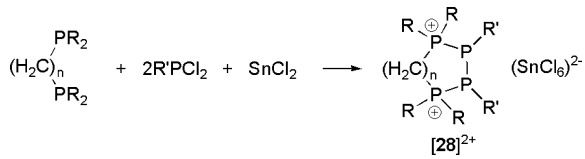

Scheme 11. Formation of *cyclic*-2-Phosphino-1,3-diphosphonium $[\mathbf{29}]^{2+}$ and 2,3-Diphosphino-1,4-diphosphonium Dications $[\mathbf{30}]^{2+}$ via Displacement Reaction of $[\mathbf{20}]^{2+}$ with dmpe and Suggested Reaction Mechanism[a]

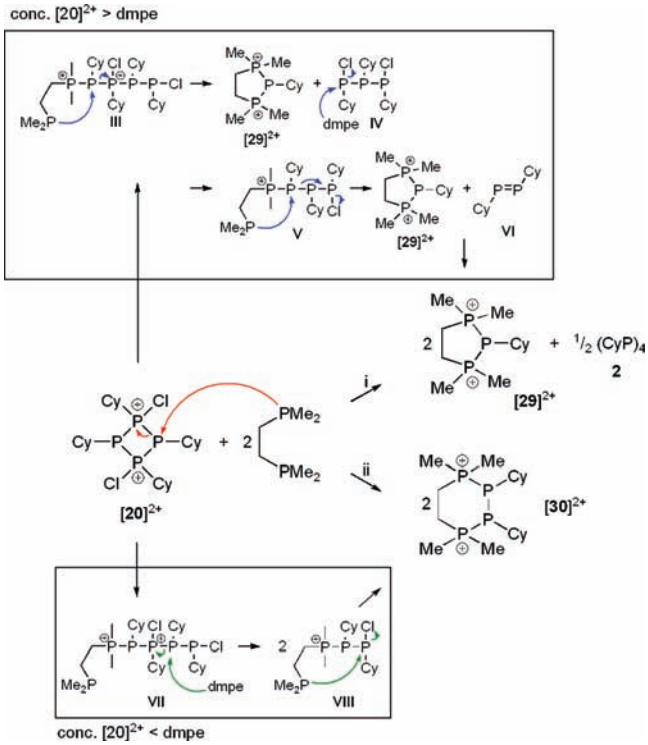

[a] (i) slow addition of dmpe, CH_2Cl_2, 0 °C, (ii) fast addition of $[\mathbf{20}][Ga_2Cl_7]_2$ to dmpe, CH_2Cl_2, RT.

ligand-stablized diphosphenium dication. In this context, Dillon and co-workers reported the reductive cycloaddition reaction of dichlorophosphines with a bidentate diphosphine to form *cyclo*-2,3-diphosphino-1,4-diphosphonium dications $[\mathbf{28}]^{2+}$ with an organic backbone (Scheme 10).[50] By analogy, when a solution of $[\mathbf{20}][Ga_2Cl_7]_2$ in CH_2Cl_2 is added rapidly to a CH_2Cl_2 solution containing 2 equiv of dmpe, a oily phase is formed which has been characterized as an equimolar mixture of the new salts $[\mathbf{29}][GaCl_4]_2$ and $[\mathbf{30}][GaCl_4]_2$ and **2**, as illustrated in Scheme 11. The oil dissolves in acetonitrile accompanied by precipitation of **2**. The clear solution exhibits the $^{31}P\{^1H\}$ NMR spectrum depicted in Figure 9, displaying AX_2 and AA′XX′

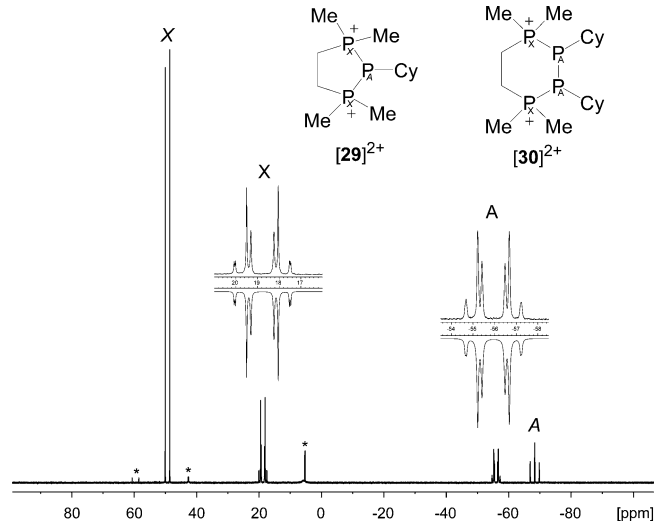

Figure 9. $^{31}P\{^1H\}$ NMR spectra (CH_3CN, C_6D_6 capillary, RT) of the redissolved precipitate of the reaction mixture of $[\mathbf{20}][Ga_2Cl_7]_2$ with dmpe according to Scheme 11 (a,ii). Signals assigned to unknown side-products are labeled with asterisks. Expansions (inset) show the experimental (up) and fitted[23] (down) spectra for cation $[\mathbf{20}]^{2+}$.

spin systems assigned to cations $[\mathbf{29}]^{2+}$ and $[\mathbf{30}]^{2+}$, respectively (Table 2). Compound $[\mathbf{30}][GaCl_4]_2$ could not be isolated, but the $^{31}P\{^1H\}$ NMR spectrum has been successfully simulated as an AA′XX′ spin system in accordance to other *cyclo*-2,3-diphosphino-1,4-diphosphonium dications[50] (Figure 9).

The reaction of dmpe with dication $[\mathbf{20}]^{2+}$ to form cations $[\mathbf{29}]^{2+}$ and $[\mathbf{30}]^{2+}$ can be interpreted according to the proposed mechanisms in Scheme 11. The initial step for both cases is the ring-opening of $[\mathbf{20}]^{2+}$ by nucleophilic attack of dmpe to form dication **III**. The subsequent reaction can now proceed in one of two ways. The dication **III** is not observed implying either fast intermolecular nucleophilic attack by a second dmpe molecule (conc. $[\mathbf{20}]^{2+}$ < dmpe) to form cation **VII** or by an intramolecular attack (conc. $[\mathbf{20}]^{2+}$ > dmpe) to form cation $[\mathbf{29}]^{2+}$ and triphosphine **IV**. Intramolecular ring-closure of cation **VII** results in the formation of dication $[\mathbf{30}]^{2+}$. Triphosphines of type **IV** are known to be highly reactive and we speculate that the reaction of a second equivalent of dmpe leads to the formation of cation **V**. Subsequent intramolecular attack according to Scheme 11 results in the formation of the second equivalent of $[\mathbf{29}]^{2+}$ and [CyP═PCy],[37] which dimerizes to give **2**. Attempts to identify the intermediates **III**−**VII** in various stoichiometric combinations of dication $[\mathbf{20}]^{2+}$ and dmpe and under various reaction conditions were unsuccessful. However, when 2 equiv of dmpe are added slowly to a cooled (0 °C) solution of $[\mathbf{20}][Ga_2Cl_7]_2$ in CH_2Cl_2, the $^{31}P\{^1H\}$ NMR spectrum of the reaction mixture reveals the stoichiometric formation of only $[\mathbf{29}][GaCl_4]_2$ and **2** (Scheme 11). The salt was isolated in high yield (85 %) as air- and moisture-sensitive colorless blocks. The solid state structure of $[\mathbf{29}]^{2+}$, shown in Figure 10, exhibits structural features that are consistent with those of derivatives previously prepared by the alkylation[51] of *cyclic* triphosphenium ions to form triphosphonium salts.[52,53] The formation of the mixture of cations $[\mathbf{29}]^{2+}$ and $[\mathbf{30}]^{2+}$ might be explained by these two competitive reactions, however, dication $[\mathbf{29}]^{2+}$ is the thermodynamically favored product. The formation of the kinetically favored dication $[\mathbf{30}]^{2+}$ results from the local

(50) Boyall, A. J.; Dillon, K. B.; Howard, J. A. K.; Monks, P. K.; Thompson, A. L. *Dalton Trans.* **2007**, 1374–1376.

(51) Dillon, K. B.; Goeta, A. E.; Howard, J. A. K.; Monks, P. K.; Shepherd, H. J.; Thompson, A. L. *Dalton Trans.* **2008**, 1144–1149.

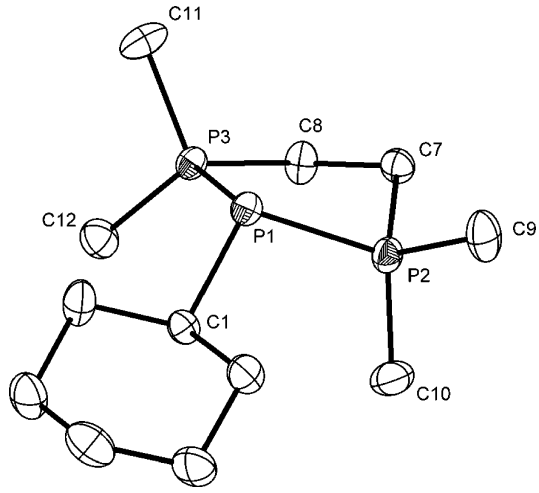

Figure 10. ORTEP plot of the molecular structure of the cation $[\mathbf{29}]^{2+}$ in $[\mathbf{29}][GaCl_4]_2$. Thermal ellipsoids with 50% probability (hydrogen atoms and counteranions are omitted for clarity). Selected bond lengths (Å) and angles (deg): P1−P2 2.191(1), P1−P3 2.214(1), P1−C1 1.873(3), P2−C7 1.806(3), P2−C9 1.792(4), P2−C10 1.795(4), P3−C8 1.815(3), P3−C11 1.787(3), P3−C12 1.783(4), C7−C8 1.535(5), P2−P1−P3 90.18(4), P2−P1−C1 104.4(1), P3−P1−C1 108.1(1), C9−P2−C10 110.6(8), C9−P2−C7 110.1(2), P1−P2−C10 116.4(1), P1−P2−C7 100.2(1), C11−P3−C12 108.6(2), C8−P3−C11 110.3(2), P1−P3−C12 117.3(1), P1−P3−C11 107.2(1), P1−P3−C8 104.4(1).

overconcentration of dmpe, since the dication $[\mathbf{20}]^{2+}$ was slowly added to the dmpe solution.

Conclusion

Reactions of tetracyclohexyl-*cyclo*-tetraphosphine $(CyP)_4$ with a source of halonium cations in the presence of GaX_3 (X = Cl, I) allows for the isolation of first *cyclo*-2-halo-1,3,4-triphosphino-2-phosphonium cations and *cyclo*-2,4-dihalo-1,3-diphosphino-2,4-diphosphonium dications as their corresponding met-

Scheme 12. Formal Retro [2 + 2] or [1 + 1 + 1′ + 1′] Reaction Channels for the Degradation of Dication $[\mathbf{20}]^{2+}$

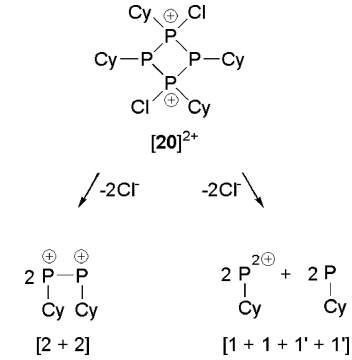

allates. Isolation of the new cations is made possible by the presence of GaX_3, which engages the halide anion and inhibits the P−P bond cleavage. In contrast to the analogous dications $[\mathbf{28}]^{2+}$ reported by Dillon and co-workers, the formation of $[\mathbf{30}]^{2+}$ represents a new approach for the generation of ligand-stabilized diphosphenium dications. Dication $[\mathbf{20}]^{2+}$ reacts with Me_3P or dmpe and dissociates formally via a retro [2 + 2] or [1 + 1 + 1′ + 1′] process (Scheme 12) releasing $[RP]^{2+}$ and $[R_2P_2]^{2+}$ fragments.

Acknowledgment. We gratefully acknowledge the Alexander von Humboldt-Foundation (Feodor Lynen Return Fellowship for J.J.W.), the FCI (Liebig scholarship for J.J.W.), the International Research Training Group (IRTG 1444, funding for R.J.D.), the European Phosphorus Science Network (PhoSciNet CM0802), the Natural Sciences and Engineering Research Council of Canada, the Killam Foundation and the Canada Research Chairs Program for funding. We thank Prof. David Emsley (McMaster University) for valuable discussion. J.J.W. thanks Prof. F. Ekkehardt Hahn (WWU Münster) for his generous support and advice.

Supporting Information Available: Crystallographic information. This material is available free of charge via the Internet at http://pubs.acs.org.

JA907693F

(52) Schmidpeter, A.; Lochschmidt, S.; Karaghiosoff, K.; Sheldrick, W. S. *J. Chem. Soc., Chem. Commun.* **1985**, 1447–1448.
(53) Ellis, B. D.; Macdonald, C. L. B. *Coord. Chem. Rev.* **2007**, *251*, 936–973, and references therein.